Supplemental Information

Rapid detection and visible light driven photocatalytic degradation of chloramphenicol in aqueous medium using $CoAl_2O_4$/rGO nanocomposite

Kamalpreet Kaur[a,#], Tarab Akhtar[a,#], Gagandeep Singh[b,#], Navneet Kaur[c,*], Narinder Singh[a,*]

[a]Department of Chemistry, Indian Institute of Technology Ropar, Rupnagar, Punjab 140001, India

[b]Chitkara College of Pharmacy, Chitkara University, Punjab 140401, India

[c]Department of Chemistry, Punjab University, Chandigarh 160014, India

 # The authors contributed equally in this work

Corresponding author's E-mail: nsingh@iitrpr.ac.in; navneetkaur@pu.ac.in

S.No.	Title
Figure S1	Linear calibration plot of CV showing the linear change in peak current of $CoAl_2O_4$-rGO/GCE respectively with increasing concentration of CAP.
Figure S2	Plot of square root scan rate vs current with error bars
Figure S3	Plot of scan rate vs current
Figure S4	Linear regression plot between log current versus log of scan rate.
Figure S5	Linear calibration plot of LSV showing the linear change in peak current with a concentration of CAP.
Figure S6	Linear calibration plot of DPV showing the linear change in peak current with a concentration of CAP.
Figure S7	Linear calibration plot of the amperometry study after successive addition of CAP.
Figure S8	(A) EIS measurements for various concentrations of CAP at rGO-$CoAl_2O_4$/GCE. (B) The calibration curve for the determination of CAP.
Figure S9	Plot of pH vs. current in 0.1 M PBS containing 120 μM solution of CAP at the $CoAl_2O_4$-rGO.
Figure S10	Correlation of pH with Ep.
Figure S11	Bar graph showing the stability of response of $CoAl_2O_4$-rGO for CAP detection with number of days.
Figure S12	Reduction peak currents of 2.5, 5, 7.5 and 10 mg $CoAl_2O_4$-rGO/GCE of 120 μM CAP in 0.1 M PBS pH 7.00 at scan rate 100 mV s^{-1}
Figure S13	Bar graph showing the stability of response of $CoAl_2O_4$-rGO for CAP detection with number of different samples.
Figure S14	EDAX analysis of rGO.
Figure S15	EDAX analysis of $CoAl_2O_4$.
Figure S16	EDAX analysis of rGO@$CoAl_2O_4$.
Figure S17	(A) The particle size distribution histogram of $CoAl_2O_4$ nanoparticles, (B) DLS histogram of $CoAl_2O_4$ nanoparticles
Figure S18	(A) Absorption spectra of CAP photocatalytic degradation under the influence of various catalysts, (B) Photocatalytic degradation efficiencies of various catalysts and (C) absorption capacities of various catalysts.
Figure S19	Reactions involving degradation of CAP using rGO@$CoAl_2O_4$.
Figure S20	Degradation products of CAP using $CoAl_2O_4$/rGO nanocomposite.

Figure S21	Schematic illustration of CAP real sample analysis.
Table 1	Real sample analysis of CAP in water
Table 2.	Comparison with literature reports for CAP detection

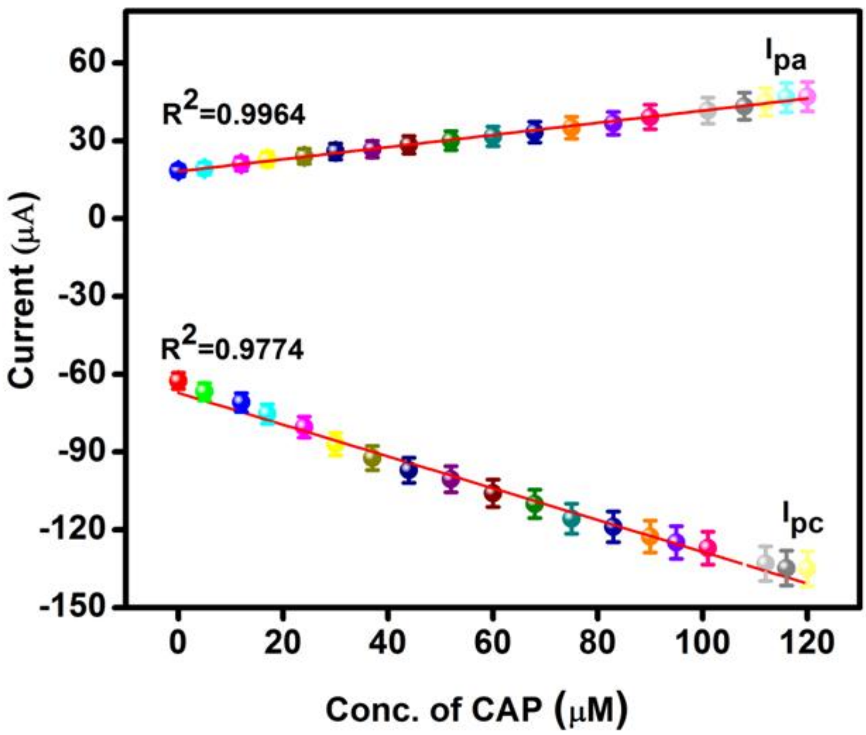

Figure S1. Linear calibration plot of CV showing the linear change in peak current of $CoAl_2O_4$-rGO/GCE respectively with increasing concentration of CAP.

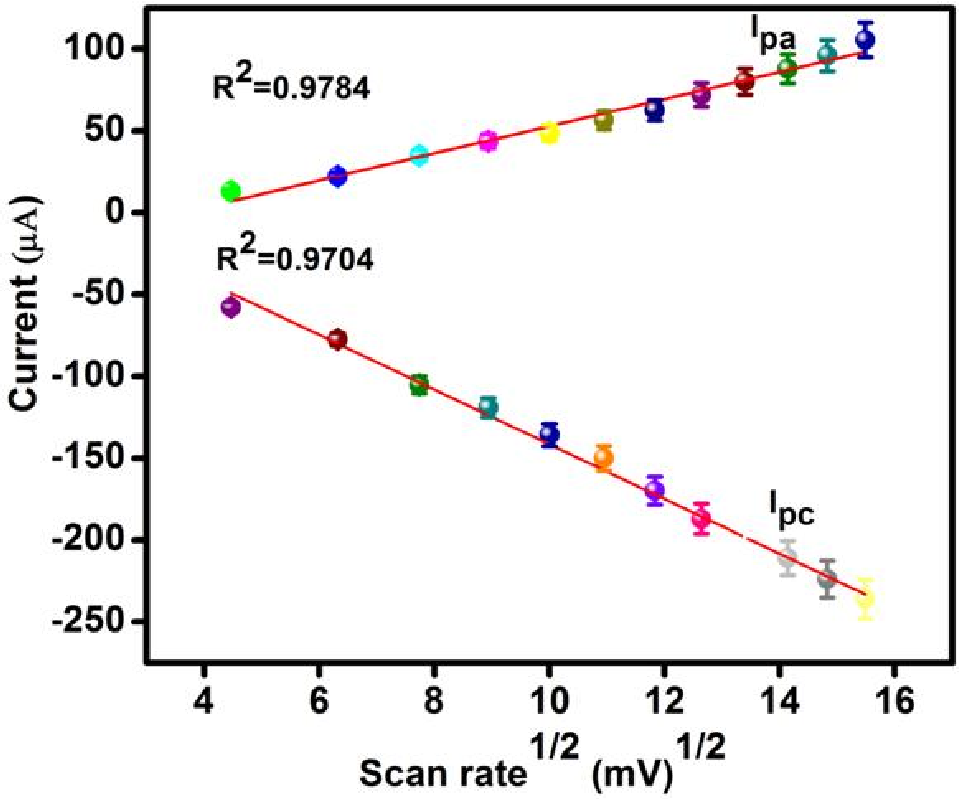

Figure S2. Plot of square root scan rate vs current with error bars

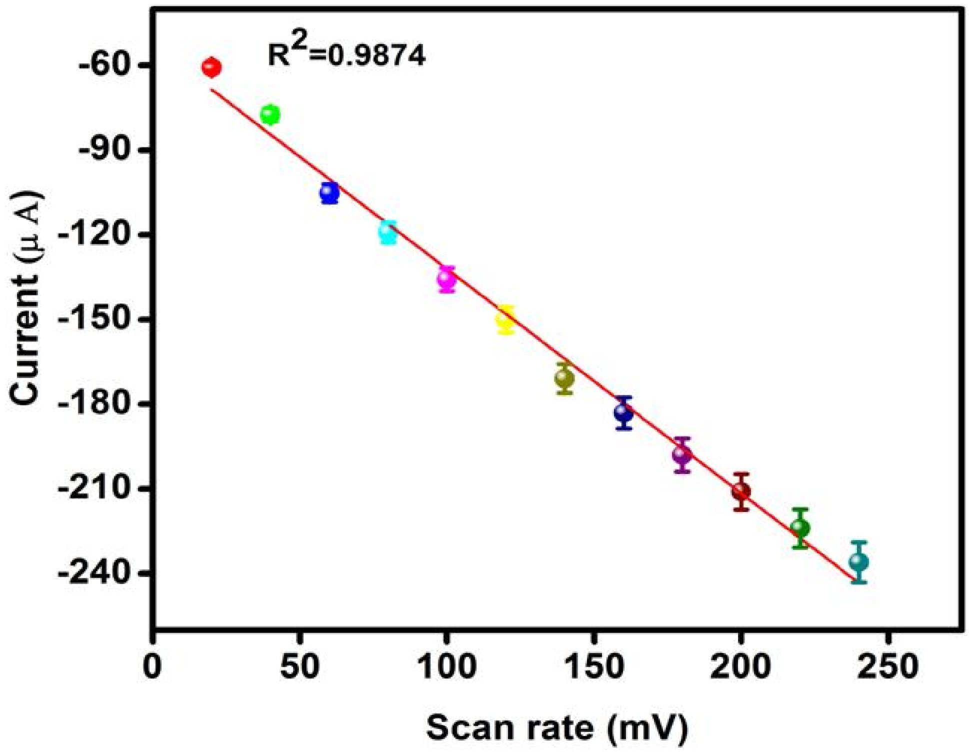

Figure S3. Plot of scan rate vs current

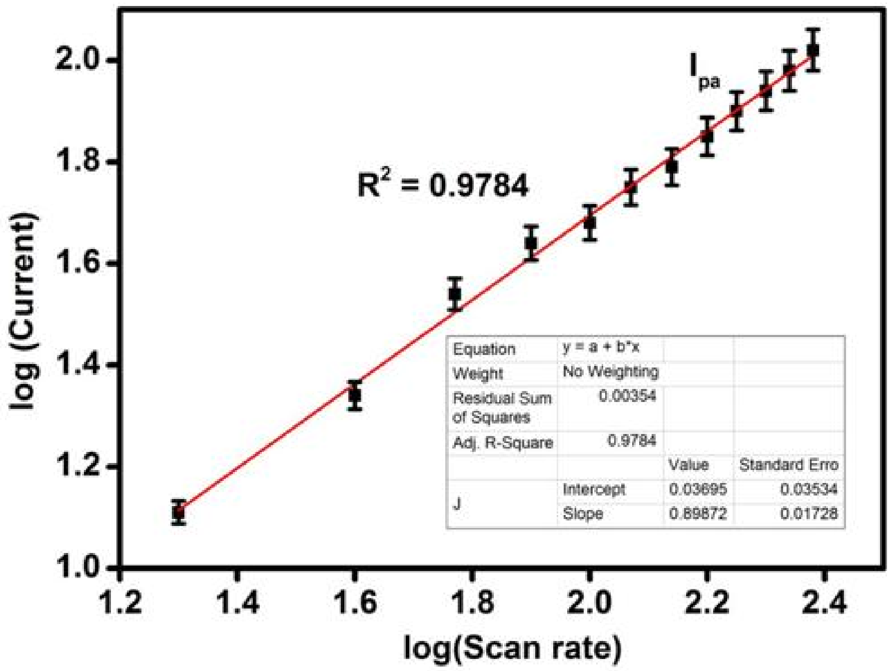

Figure S4. Linear regression plot between log current versus log of scan rate.

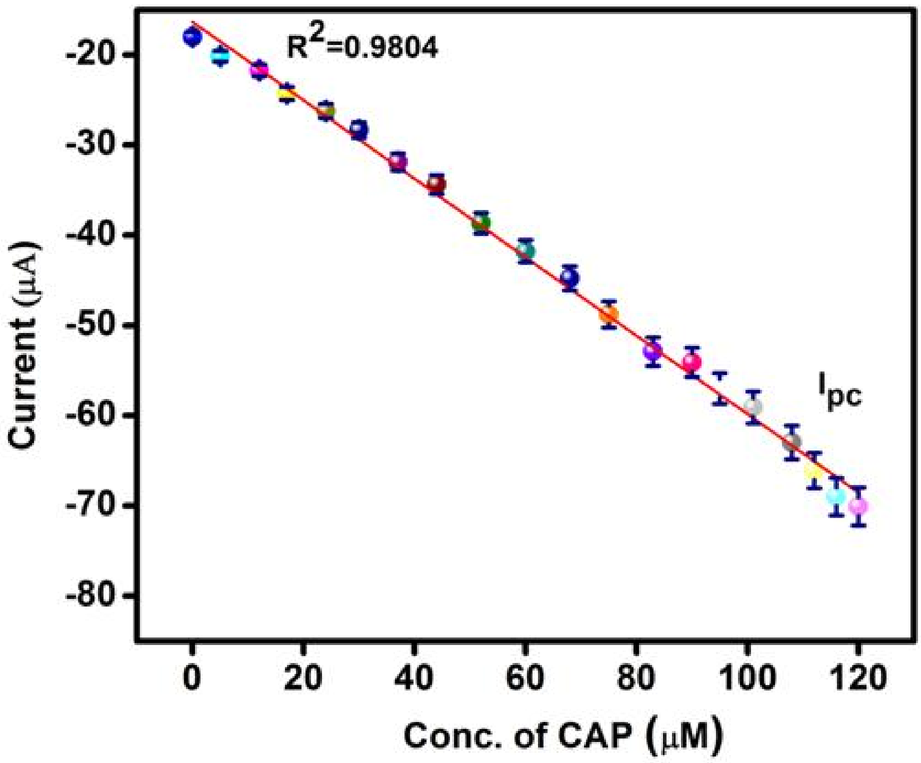

Figure S5. Linear calibration plot of LSV showing the linear change in peak current with a concentration of CAP.

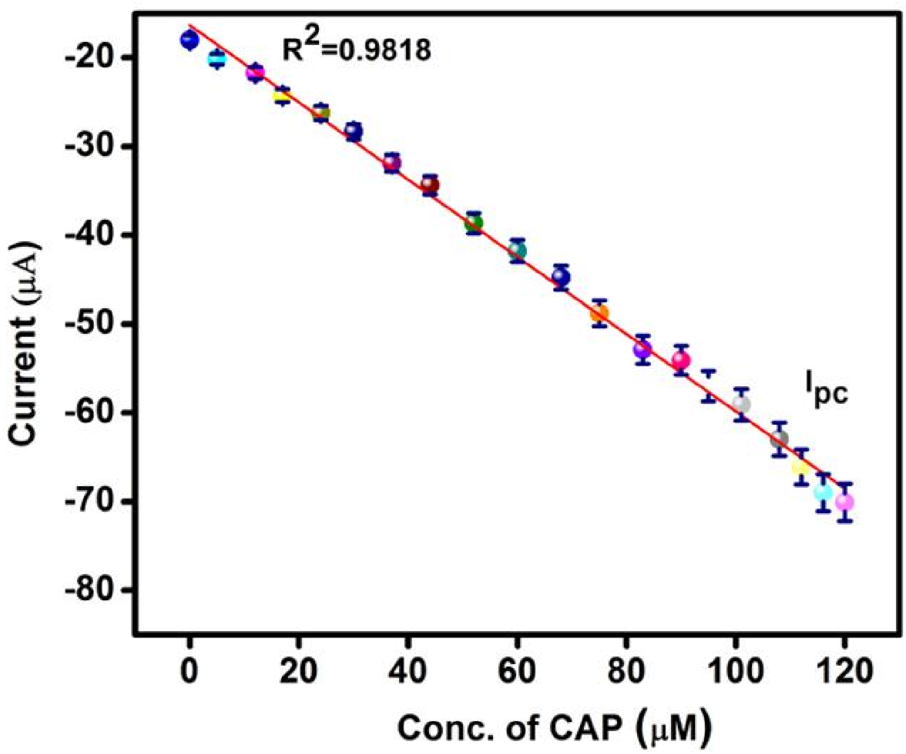

Figure S6. Linear calibration plot of DPV showing the linear change in peak current with a concentration of CAP.

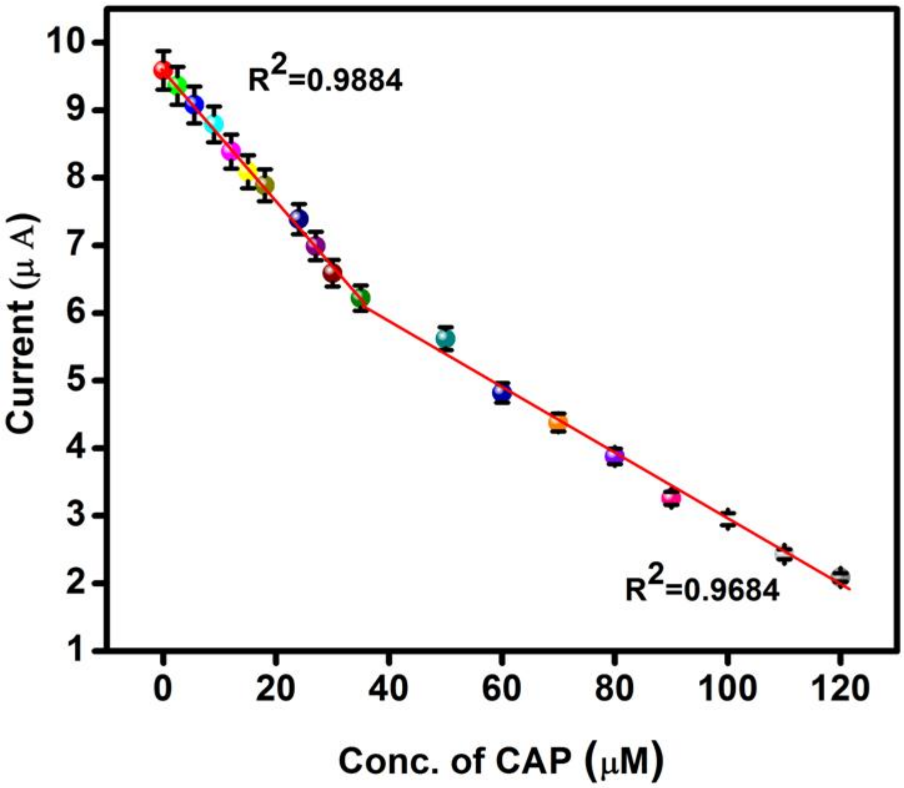

Figure S7. Linear calibration plot of the amperometry study after successive addition of CAP.

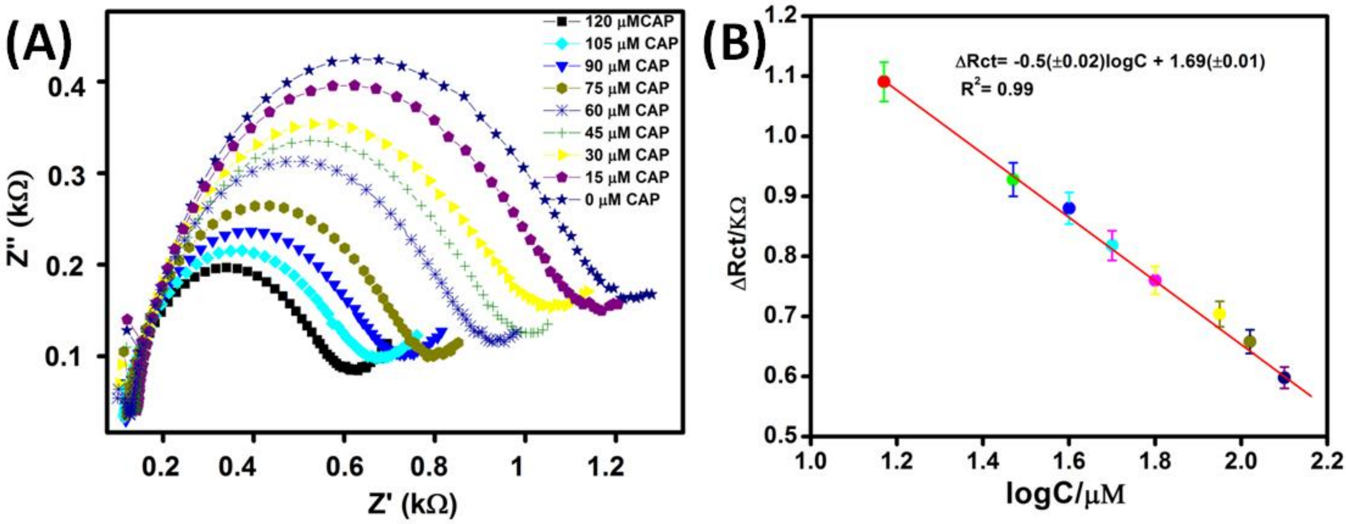

Figure S8. (A) EIS measurements for various concentrations of CAP at rGO-$CoAl_2O_4$/GCE. (B) The calibration curve for the determination of CAP.

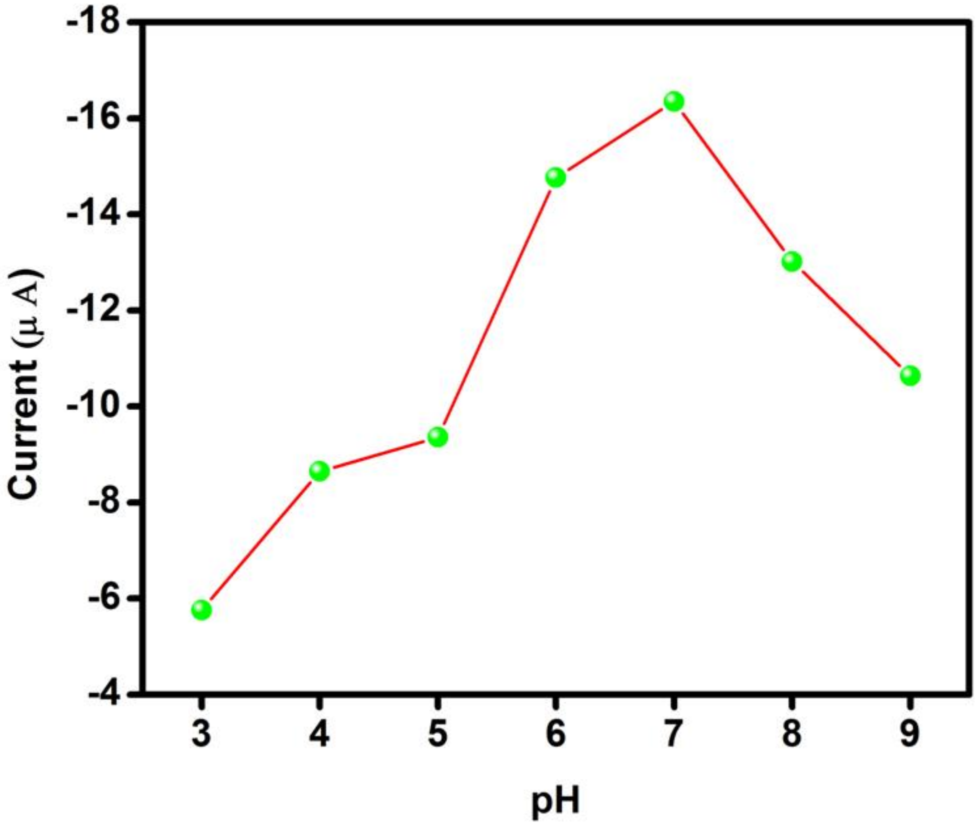

Figure S9. Plot of pH vs. current in 0.1 M PBS containing 120 μM solution of CAP at the $CoAl_2O_4$-rGO.

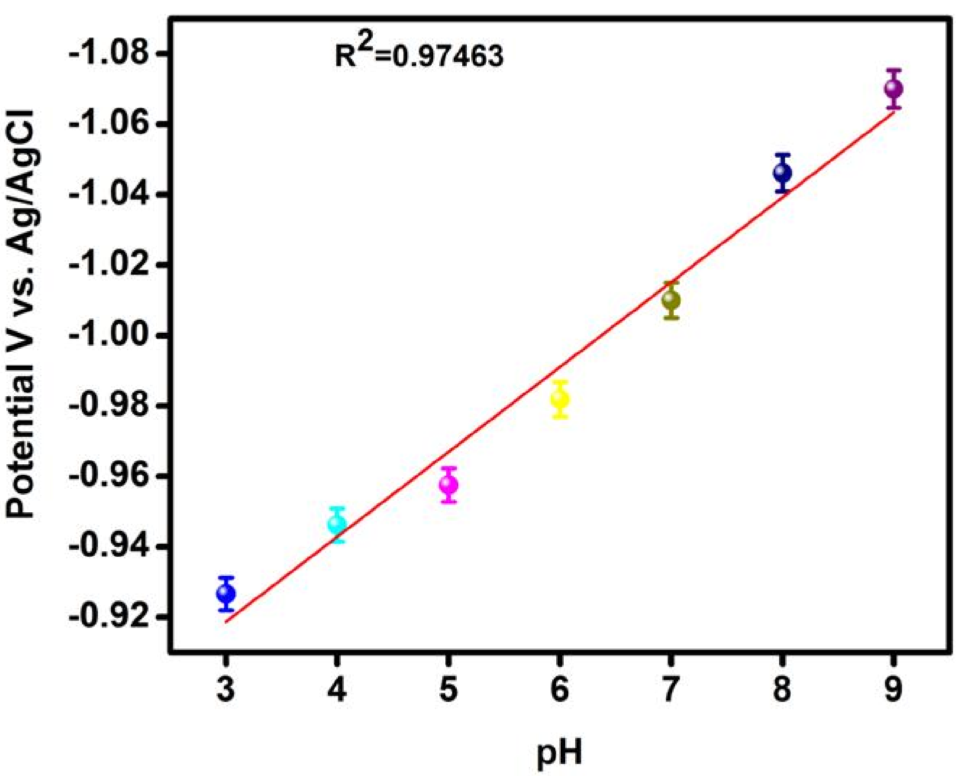

Figure S10. Correlation of pH with Ep.

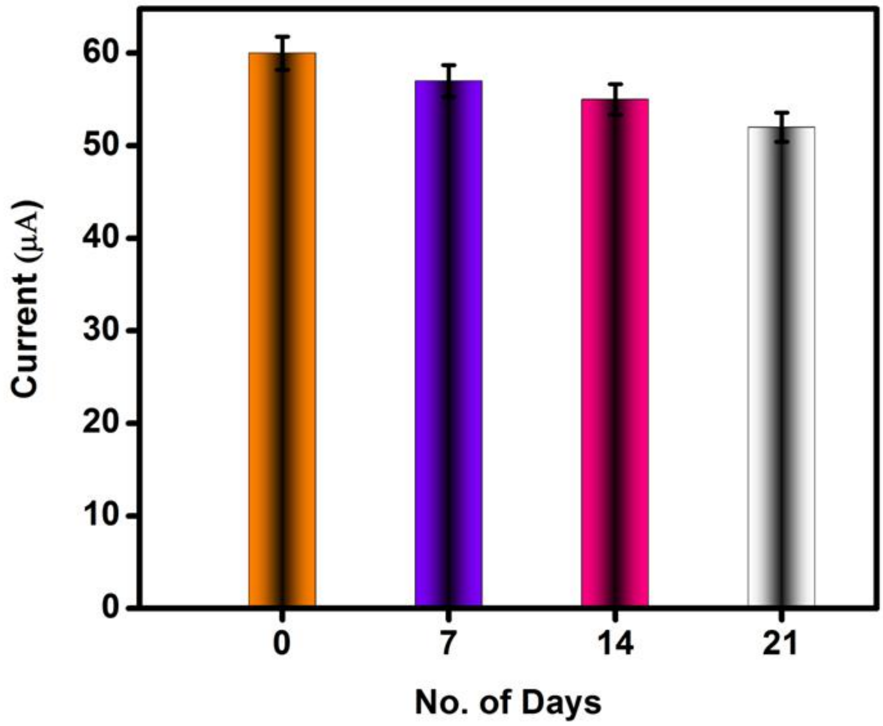

Figure S11. Bar graph showing the stability of response of $CoAl_2O_4$-rGO for CAP detection with number of days.

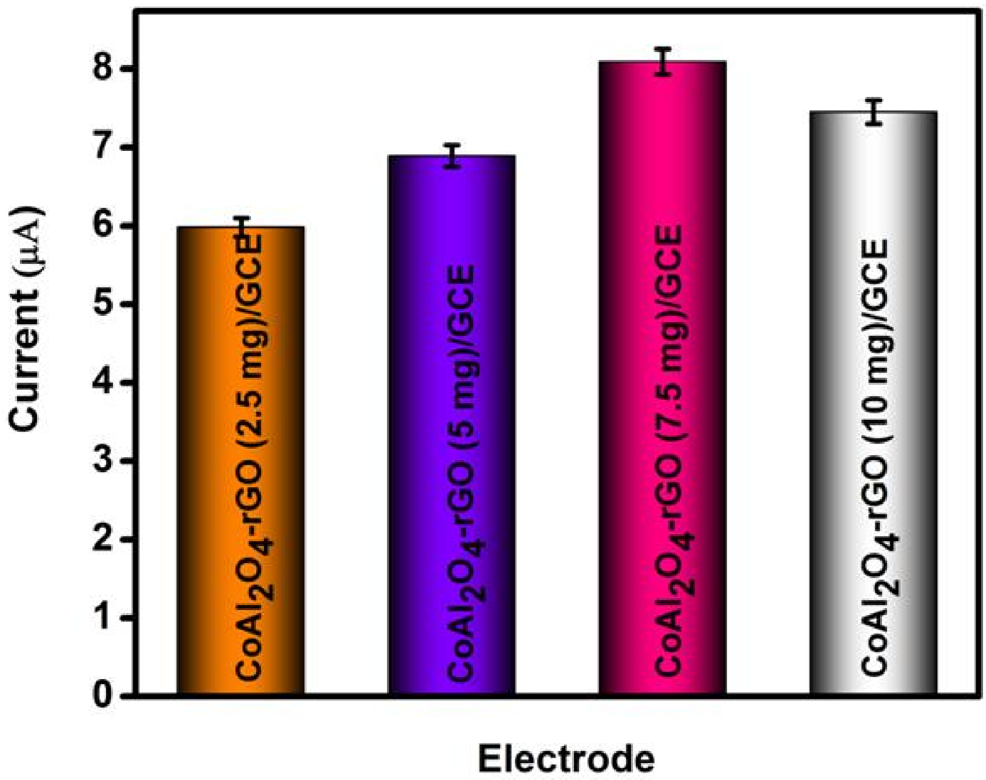

Figure S12. Reduction peak currents of 2.5, 5, 7.5 and 10 mg $CoAl_2O_4$-rGO/GCE of 120 μM CAP in 0.1 M PBS pH 7.00 at scan rate 100 mV s^{-1}

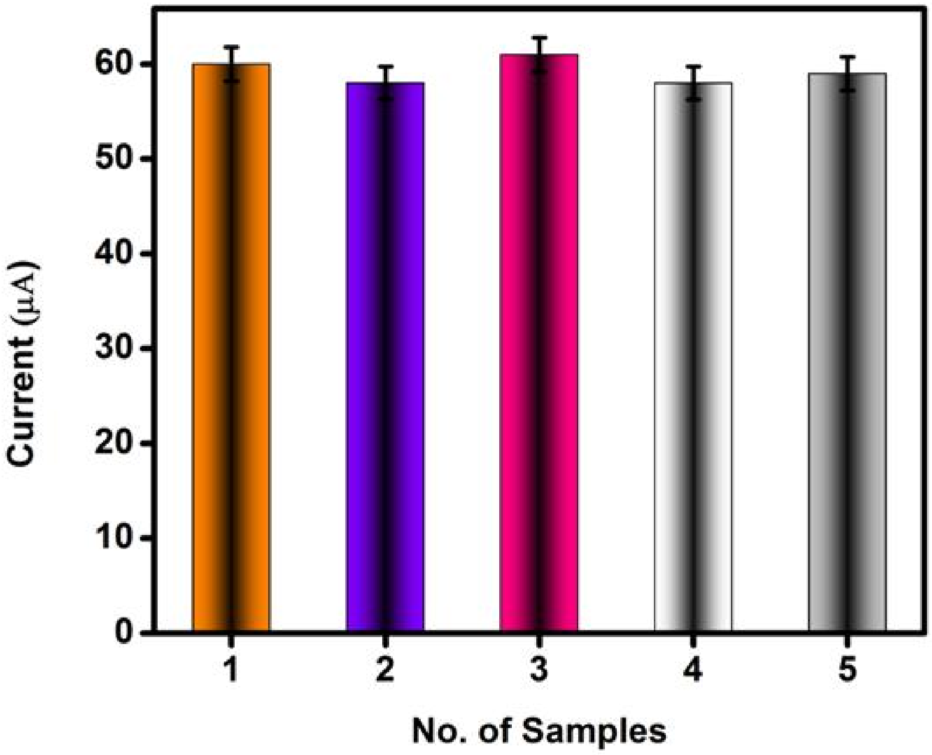

Figure S13. Bar graph showing the stability of response of $CoAl_2O_4$-rGO for CAP detection with number of different samples.

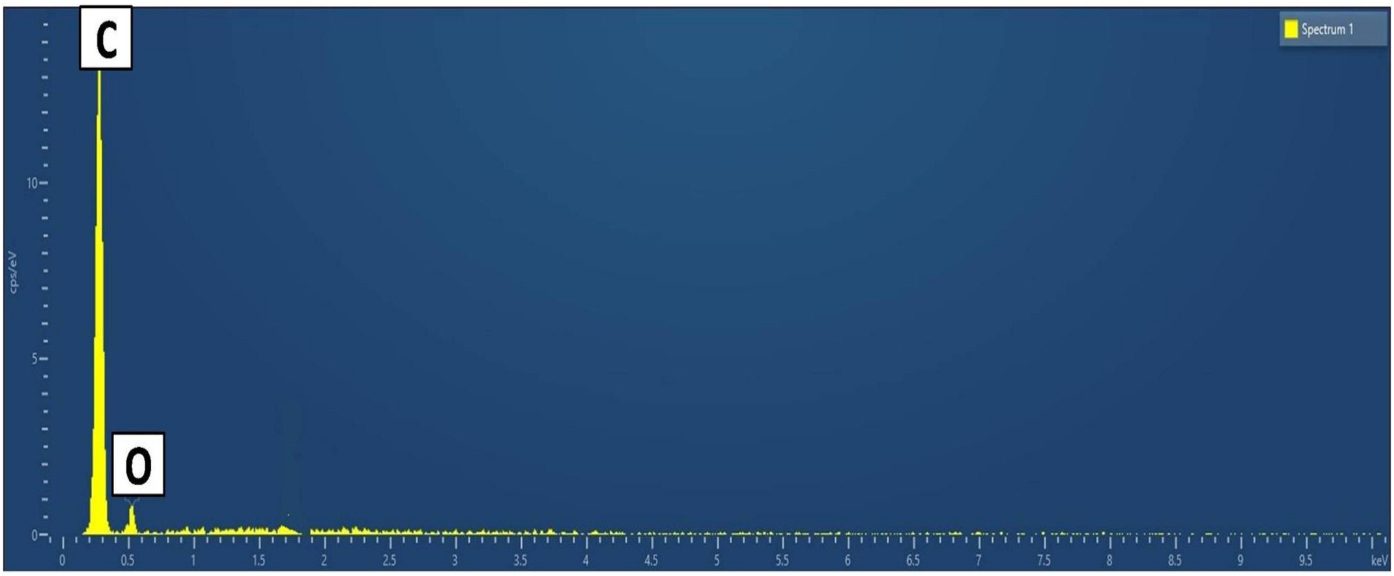

Figure S14. EDAX analysis of rGO.

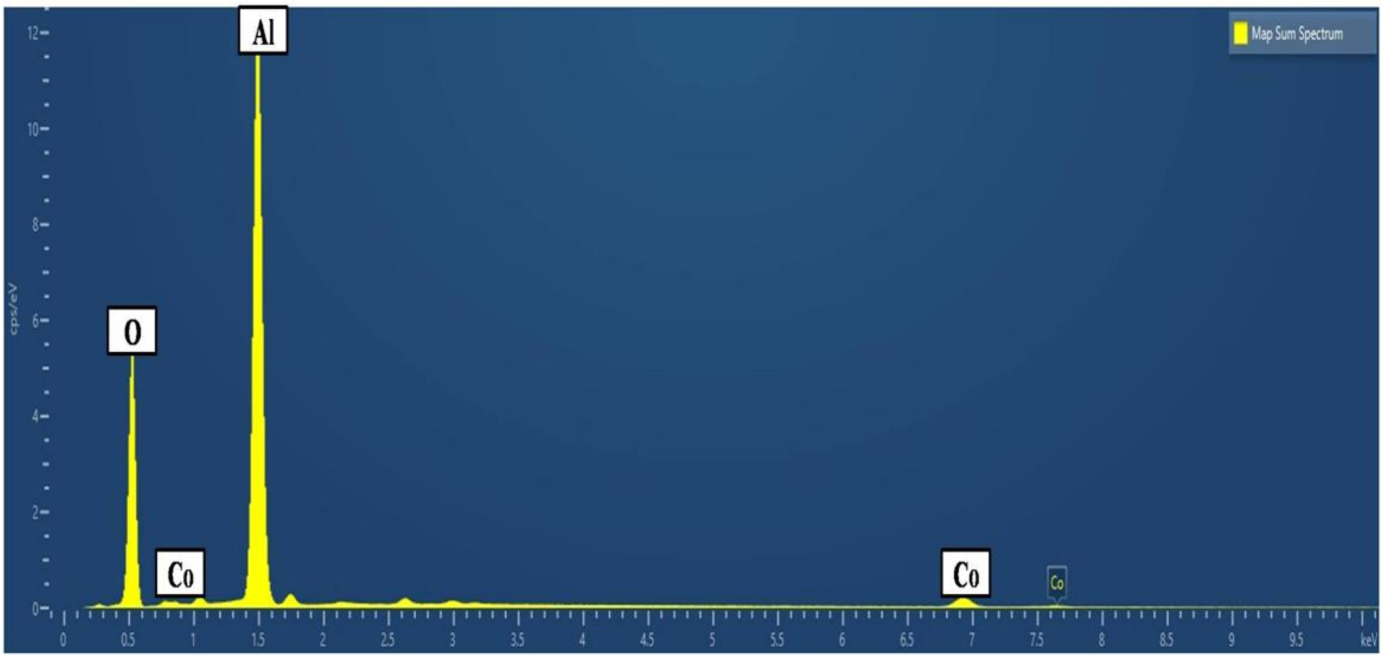

Figure S15. EDAX analysis of $CoAl_2O_4$.

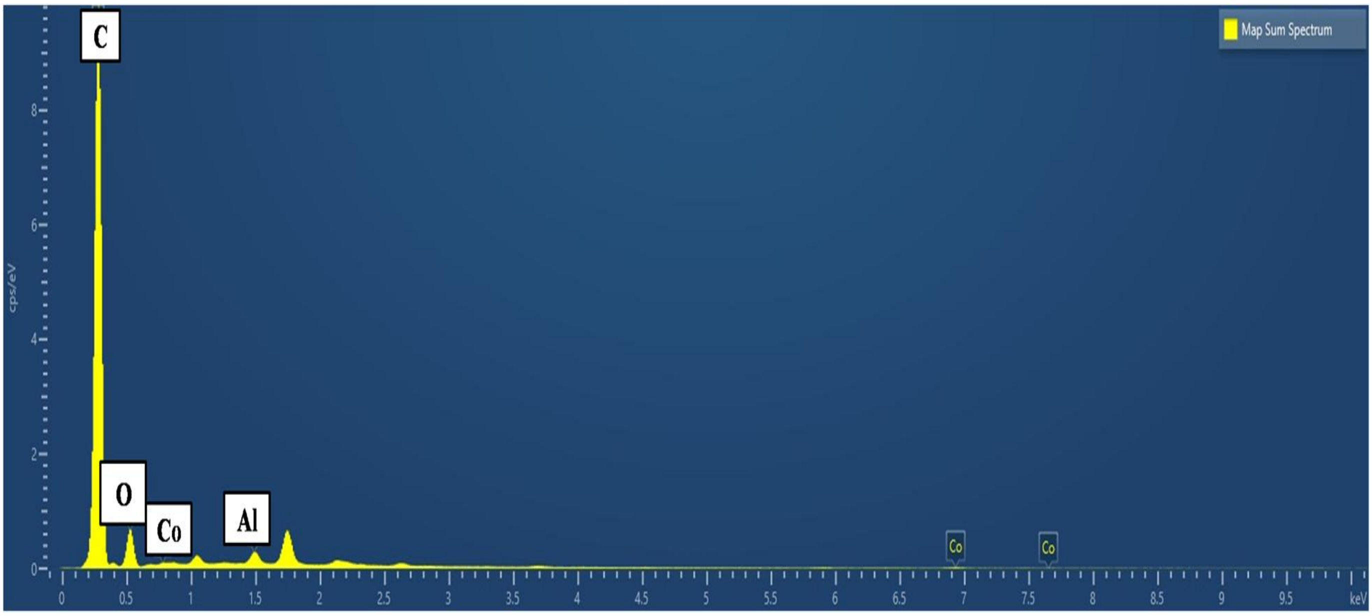

Figure S16. EDAX analysis of $rGO@CoAl_2O_4$.

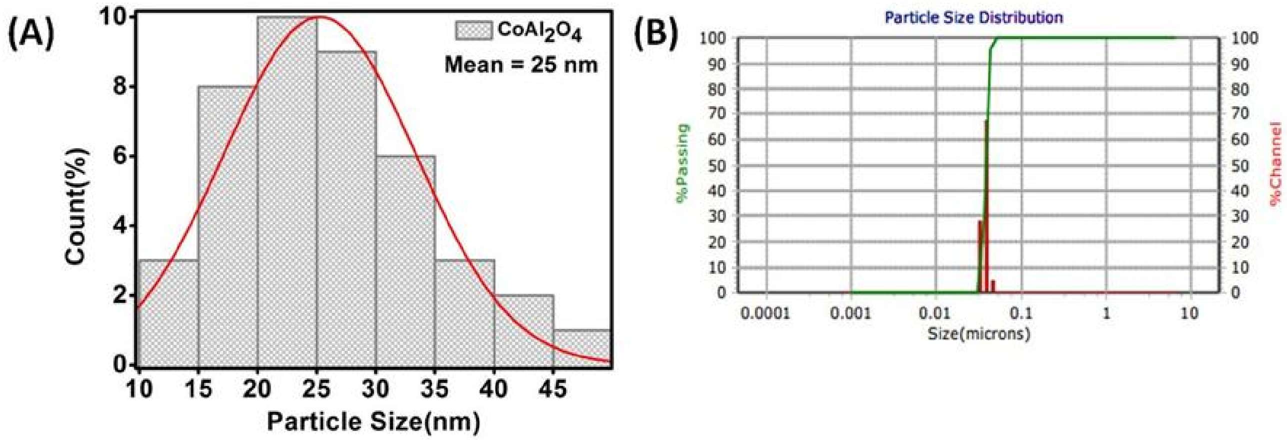

Figure S17. (A) The particle size distribution histogram of $CoAl_2O_4$ nanoparticles, (B) DLS histogram of $CoAl_2O_4$ nanoparticles

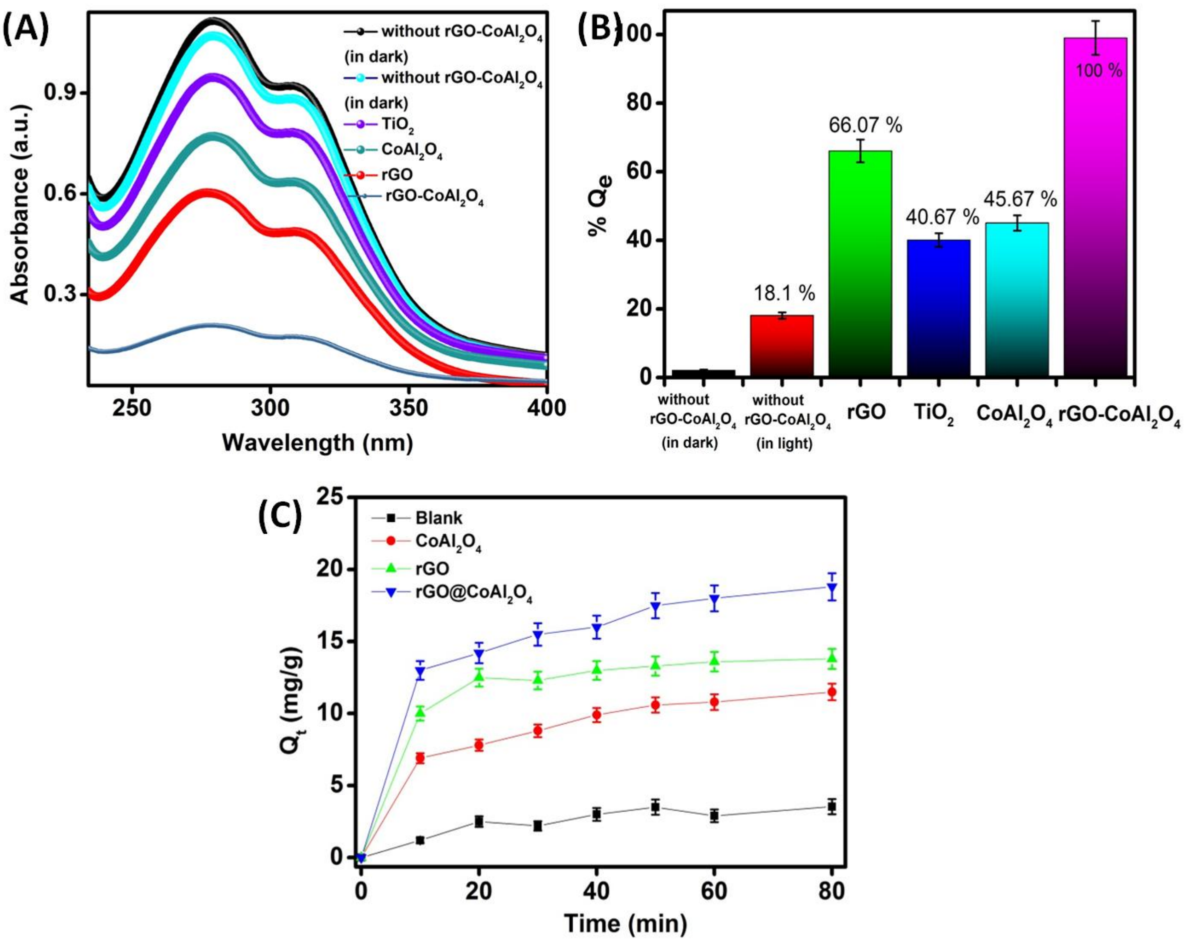

Figure S18. (A) Absorption spectra of CAP photocatalytic degradation under the influence of various catalysts, (B) Photocatalytic degradation efficiencies of various catalysts and (C) absorption capacities of various catalysts.

$$rGO@CoAl_2O_4 + h\nu \longrightarrow CoAl_2O_4\,(h^+ + e^-)$$
$$CoAl_2O_4\,(e^-) \longrightarrow rGO\,(e^-)$$
$$e^- + O_2 \longrightarrow O_2^{\cdot -}$$
$$h^+ + H_2O \longrightarrow HO^{\cdot} + H^+$$
$$OH^{\cdot} + O_2^{\cdot -} + CAP \longrightarrow \text{Degradation products}$$

Figure S19. Reactions involving degradation of CAP using rGO@$CoAl_2O_4$.

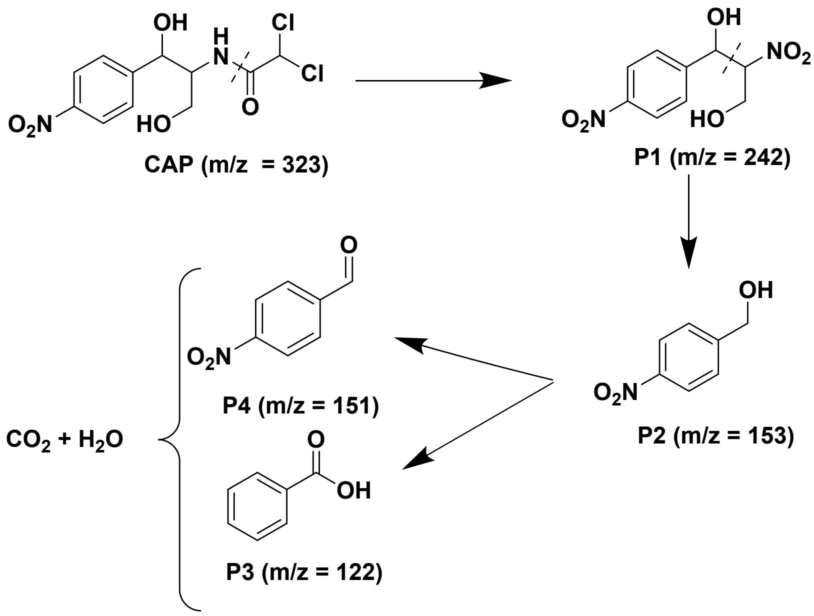

Figure S20. Degradation products of CAP using $CoAl_2O_4$/rGO nanocomposite.

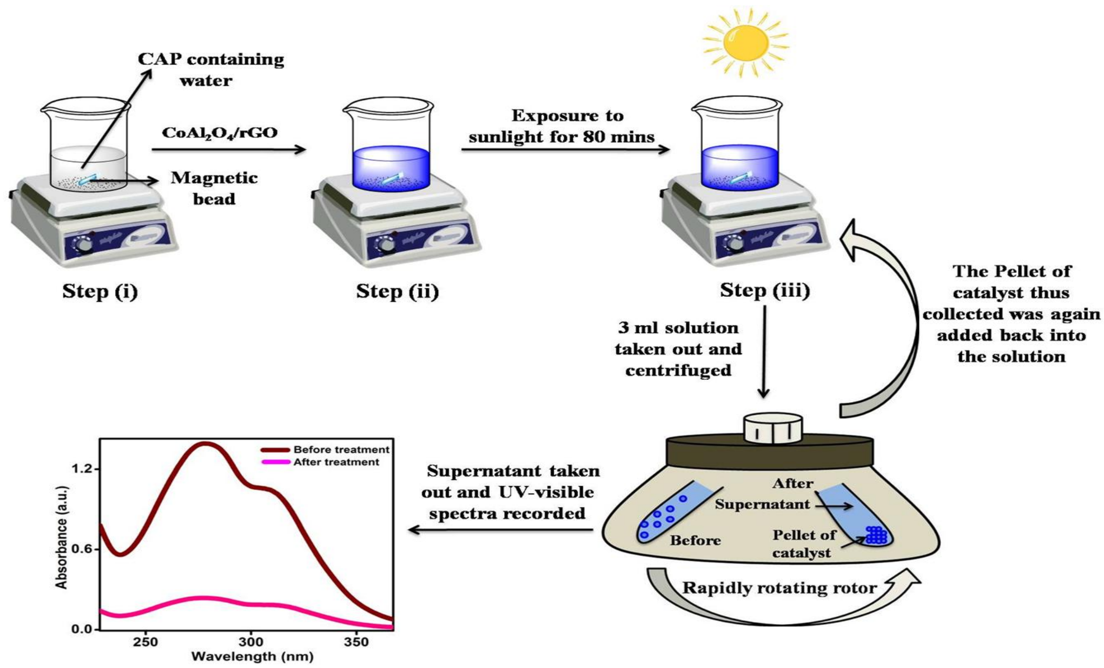

Figure S21: Schematic illustration of CAP real sample analysis.

Real sample analysis of CAP in water

Table 1.

Sample	Added/10^{-6} mol/L	Found/10^{-6} mol/L	RSD (%)	Degradation (%)
River water	10.00	9.18	0.83	91.80
	25.00	24.19	2.07	96.76
Tap water	10.00	9.89	0.75	98.90
	50.00	50.55	2.08	101.10
Pharmaceutical Sewage wastewater	10.00	10.36	0.43	103.6
	25.0	25.19	1.05	100.76

Table 2.
Comparison with literature reports for CAP detection

S.No.	Probe	Detection method	Application	Detection Limit	Linear range	References
1.	Mn_3O_4 nanoparticles for detection of chloramphenicol	Electrochemical sensor	Milk samples	0.008 µM	0.007-0.013 µM	1
2.	GCE modified with CS-MWCNTs electro-polymerization for detection of chloramphenicol	Electrochemical sensor	Milk samples	3.3×10^{-2} µM	0.1-1000 µM	2
3.	MIP/Uio-66@CDs/GCE for detection of chloramphenicol	Electrochemical Impedance Spectroscopy (EIS)	Water samples	61×10^{-9}µM	40×10^{-9} µM -61×10^{-9} µM	3
4.	CdS0.75Se0.25@oligopeptide quantum dots for detection of chloramphenicol	Fluorescent spectroscopy	Milk samples	0.89 µg/L	3.13 to 500 µg/L	4
5.	MIP-functionalized rGO for adsorption and detection of chloramphenicol	Electrochemical detection	Honey samples	0.204 µM	0.1 µM – 1.2 µM	5

6.	Sn/rGO/SPCE (Screen printed electrode) for detection of chloramphenicol	Electrochemical detection	Milk, honey samples	0.2 μM	0.5–30 μM	6
7.	Ag nanoparticles for detection of chloramphenicol	Surface-enhanced Raman scattering (SERS)	Food samples	10−5 µg/mL	102 to10^{-5} µg/mL	7
8.	$AuNPs/MoS_2/TiO_2$ for detection of Chloramphenicol	Photochemical aptasensor	Milk samples	0.5 pM	0.3-0.5 pM	8
9.	**$CoAl_2O_4$-rGO for removal as well as detection of chloramphenicol**	**Electrochemical detection**	**Water samples**	**13.5 nM**	**3.4-13.5 nM**	**This work**

References

1. R. Nehru, S. Gnanakrishnan, C.-W., Chen, C.-D, Dong, *ACS Appl. Nano Mater.,*2023, **6,** 1235–1249.

2. L. Geng, J. Huang, H. Zhai, Z. Shen, J. Han, Y. Yu, H. Fang, F. Li, X. Sun, Y. Guo, *Microchemical Journal,*2022, **182,** 107887.

3. L. Bu, X. Chen, Q. Song, D. Jiang, X. Shan, W, Wang, Z. Chen, *Microchemical Journal,*2022, **179,** 107459.

4. X. Xu, Y. Yang, H. Jin, B. Pang, R. Yang, L.Yan, C. Jiang, D. Shao, J. Shi, *ACS Sustainable Chem. Eng.,*2020, **8**, 6806–6814.

5. T. N. T. Nguyen, N. Thi Pham, D.-H . Ngo, S. Kumar, X. T. Cao,*ACS Omega,*2023**, 8** , 25385–25391.

6. S. Bunnasit, K. Thamsirianunt, R. Rakthabut, K. Jeamjumnunja, C. Prasittichai, W. Siriwatcharapiboon, *ACS Appl. Nano Mater.,*2024**, 7,** 267–278.

7. H. Li, W. Geng, M. M. Hassan, M. Zuo, W. Wei, X. Wu, Q. Ouyang, Q. Chen, Q. *Food Control,* 2021, ***128*****,** 108186.

8. C. Zhao, T. Jing, M. Dong, D. Pan, J, Guo, J. Tian, M. Wu, N. Naik, M. Huang, Z. Guo, *Langmuir,* 2022, ***38*****,** 2276–2286.